ANATOMO-FUNCTIONAL CHARACTERISATION OF THE HUMAN "HAND-KNOB": A DIRECT ELECTROPHYSIOLOGICAL STUDY

List of Authors: Viganò L.[#1], Fornia L.[#2], Rossi M.[1], Howells H.[2], Leonetti A.[2], Puglisi G.[2], Conti Nibali M.[1], Bellacicca A[2], Grimaldi M.[3], Bello L.[1], Cerri G.[2]

1) Neurosurgical Oncology Unit, Department of Oncology and Haemato-Oncology, Università degli Studi di Milano, Humanitas Research Hospital, IRCCS, Milano, Italy

2) Laboratory of Motor Control, Department of Medical Biotechnologies and Translational Medicine, Università degli Studi di Milano, Humanitas Research Hospital, IRCCS, Milano, Italy

3) Neuroradiology Unit and Neuro Center, Humanitas Research Hospital, IRCCS, Rozzano, Italy

# Equally contributed

Abstract

The cortical area within the human primary motor cortex (M1) that hosts the representation of the hand and fingers is known as the 'hand-knob' and is essential for voluntary hand movement. The anatomo-functional heterogeneity described within the monkey primary motor cortex (M1) in a rostro-caudal direction suggests an internal subdivision in two sectors originating different systems of connections to the spinal cord. Direct investigation of the human hand-knob has been prevented, so far, by methodological constraints. The unique setting of brain tumour resection with the brain mapping technique in awake patients enables direct electrophysiological investigation of the functional properties of the human hand-knob. Motor-evoked potentials (MEPs) elicited by Direct Electrical Stimulation (DES) at high frequency (HF-DES) delivered along the hand-knob in rostro-caudal direction, i.e. from the central to the precentral sulcus, were recorded from the hand/arm muscles in patients at rest. The sites located near the precentral sulcus identified with HF-DES were then stimulated with low-frequency DES (LF-DES) during a hand manipulation task (HMt) to assess whether DES affected task execution. From the stimulated sites, corticofugal projections and U-shaped tracts connecting with adjacent gyri were traced using diffusion tensor and spherical deconvolution tractography. Analysis of MEPs showed a rostro-caudal gradient of cortical excitability along the hand-knob (the rostral sector being less excitable). Stimulation of rostral sites during the HMt impaired the task by inducing dysfunctional recruitment or, alternatively, suppression of distal muscles. Diffusion tractography showed different patterns of rostro-caudal connectivity for the U-shaped tracts. Overall data suggests, in humans, the anatomo-functional subdivision of the human hand-knob in two sectors, possibly subserving different roles in motor control.

1. INTRODUCTION

The cerebral cortex within the precentral gyrus (PreCG), hosting the primary motor area (M1), plays an essential role in execution of voluntary movement. By using intraoperative direct electrical stimulation (DES), Penfield and Boldrey in 1937 demonstrated that a somatotopic representation of the body, the so-called *motor homunculus*, exists along the human precentral gyrus.

The representation of the hand in the primary motor area (M1) is prevalently localised in a specific segment of the precentral gyrus, called the 'hand-knob' due to its visible omega or epsilon shaped bulge in axial MR images (Yousry et al. 1997, Boling et al. 1999, Caulo et al. 2007). This region corresponds with the *pli de passage fronto-pariétal moyen* described by Broca (Broca 1888). Interestingly, cytoarchitectonic investigation of the human hand-knob revealed a subdivision, along the rostro-caudal direction, in different architectonic districts suggested to subserve different aspects of motor control (Geyer et al. 1996; Binkofski et al. 2002; Bastiani et al. 2016; Glasser et al. 2016). Amiez and Petrides (2018) recently confirmed a crucial role of the caudal region in the control of simple hand movements and suggested the most rostral region, corresponding to the dorsal portion of the superior precentral sulcus, to be involved in the selection of hand movements. There are reasonable grounds for this hypothesis, given the considerable evidence from non-human primate studies using intracortical micro-stimulation (ICMS), cytoarchitectonic analysis and anatomical tracers. These studies provide evidence of a strict correlation between architectonic features of different M1 subsectors and their specific roles in motor control (Strick & Preston 1982; Rathelot & Strick 2008; Witham et al., 2016). Precisely, the rostral and caudal subsectors of M1 hand region may exert different roles in motor control through different corticospinal connections. The caudal sector of M1 (the so-called "new-M1"), incorporating the bank of the central sulcus, shows dense cortico-motoneuronal (CM) projections whereas the rostral sector (the so-called "old-M1") shows very few CM projections (Rathelot & Strick 2008; Witham et al. 2016). Coherently with this structural evidence, ICMS of the two sectors evokes Excitatory Post-Synaptic Potentials (EPSPs) with different features: both sectors indeed elicit long latency monosynaptic potentials, but only the new-M1 shows fast-monosynaptic responses (Witham et al. 2016).

In addition to the different corticospinal connections, the two sectors might act through different cortico-cortical networks. In the Old World monkey, although a clear network for fine control of hand

movements has been described (Borra et al. 2017), no available data at present sheds light on a possible differentiation in cortical connectivity between the 'new-M1' and the 'old-M1'. However, in the New World monkey, in which the whole M1 is unfolded on the convexity, a different pattern of cortico-cortical connectivity has been shown in the rostro-caudal direction: the rostral M1 is primarily connected with premotor areas, especially the caudal portion of dorsal premotor (dPM) and ventral premotor (vPM) cortex, while the caudal M1 is primarily connected with somatosensory cortices (Stepniewska et al. 1993, 2006; Dea et al. 2016). In humans, a system of U-shaped fibres connecting the M1 hand motor area both to premotor and postcentral regions (Rosett 1933; Catani et al. 2012; Thompson et al. 2017) has been highlighted but no conclusive evidence of a different connectivity between M1 subsectors has yet been shown.

Despite attempts to characterise functional properties of the human M1 with indirect techniques (Kleinschmidt et al. 1997; Meier et al. 2008), a direct electrophysiological approach with high spatial resolution is the best approach currently available for investigating the anatomo-functional rostro-caudal organization within the human hand-knob. We addressed this issue by analysing the neurophysiological data recorded intraoperatively in patients undergoing awake surgery for brain tumour resection with the aid of the Brain Mapping Technique and Direct Electrical Stimulation (DES). The analysis focused on data recorded when stimulating the hand-knob sector in the right hemisphere of 17 selected patients adopting a multimodal approach, i.e. by combining the analysis of data obtained during mapping with High Frequency Stimulation at rest (HF-DES-Rest), Low Frequency Stimulation during a voluntary hand manipulation task (HMt, LF-DES-HMt) and neuroimaging data by performing diffusion tractography to explore the white matter anatomy using Diffusion Tensor (DTI) and High Angular Resolution Diffusion Imaging (HARDI). During surgery, the choice of a HF or LF-DES paradigm to be used to perform brain mapping depends on the clinical context (critically the specific neurological function to be preserved and the clinical conditions that may affect excitability of the patient's brain tissue). By inducing a clear motor output, Motor Evoked Potentials (MEPs), HF-DES is effective in mapping primary and non-primary motor areas/pathways (Bello et al. 2014; Fornia et al. 2016). LF-DES, on the other hand, may elicit a motor output when applied to motor areas, although with differences with respect to HF-DES (Bello et al. 2014). Additionally, LF-DES, by transiently interfering with the neuronal activity of a small amount of tissue below the probe, affects the execution of specific tasks (Bello et al. 2014; Rossi et al. 2018) when applied on neural networks underlying their execution.

Analysis of the intraoperative data allows for specific investigation of the precentral gyrus focusing on two subsectors, the sector close to the central sulcus, here defined as the *caudal hand-knob*, and

the sector close to the precentral sulcus, here defined as the *rostral hand-knob*. Analysis of the motor output elicited by HF-DES applied on the hand-knob in a resting condition was performed to evaluate whether differences in MEP features correlated with stimulation of different subsectors. The stimulation parameters and MEP amplitude were used to establish differences in the cortical excitability between the two sectors. The hypothesis was that a gradient of excitability in the rostro-caudal direction within the hand knob exists, which points to a functional subdivision of this sector. We previously demonstrated that the quantitative analysis of the same MEPs parameters is reliable in differentiating between two functionally distinct regions within the precentral gyrus (ventrolateral premotor cortex and M1) (Fornia et al. 2016).

When appropriate for the clinical context (Bello et al 2014), brain mapping requires LF-DES-HMt whereby the precentral gyrus is stimulated while the patient performs a dedicated voluntary hand-manipulation task (HMt), an intraoperative tool efficient in preventing post-operative apraxia (Rossi et al 2018). The HMt requires adequate coordination of muscles synergies to achieve the appropriate hand-object interaction to correctly perform the task. Analysis of the interference during HMt execution was focused on impairment of hand movement (an observed behavioural outcome) and on electrical activity (EMG) of the muscles primarily involved in HMt execution. Analysis of the specific features characterizing the effect of DES on task execution was aimed at providing insight as to the role of this sector in motor control for skilled hand-object interaction.

Finally, we evaluated patterns of white matter connectivity of the precentral gyrus in a subset of six patients: specifically, the corticofugal connections and the U-shaped connections surrounding the precentral sulcus, and those connected with the postcentral gyrus (Catani et al. 2012) were studied to assess whether differences in anatomical connectivity may correspond with rostro-caudal functional differences occurring in the hand-knob, as highlighted by our electrophysiological results.

2. MATERIAL AND METHODS

The main aim of the present study was to investigate the human precentral gyrus, specifically focusing on the anatomo-functional properties of the hand-knob along the rostro-caudal direction. To this end, we performed a multimodal analysis of electrophysiological and neuroimaging data recorded in patients undergoing awake surgery for brain tumour resection in the right hemisphere.

According to standard procedure, the surgical resection was performed according to functional boundaries by means of the brain mapping technique and Direct Electrical Stimulation (DES) (Bello et al. 2014). All the patients performed the entire standard brain mapping procedure, which consists of the combination of High Frequency DES and Low Frequency DES (so defined according to the

frequency of pulses in the delivered stimulating train, see Bello et al. 2014), aimed at the individuation of the safety entry point and at the preservation of eloquent cortical and subcortical structures.

The strict inclusion criteria allowed us to select and investigate, in 17 patients, two cortical subsectors of hand-knob, the caudal ones (close to the central sulcus) and the rostral ones (close to the precentral sulcus). Two stimulation paradigms were available during the procedure: the High Frequency and the Low Frequency stimulation and, based on the clinical context (Bello et al. 2014) one or both (see Table 1) paradigms were delivered during the awake period of the procedure.

1) <u>High Frequency Monopolar Stimulation at rest (HF-DES-Rest),</u> i.e. in absence of voluntary movement, was applied at the beginning of the procedure. HF-DES-Rest was used to explore the precentral hand-knob in the rostro-caudal direction to identify the most excitable cortical site based on the occurrence and amplitude of the Motor Evoked Potentials (MEPs) evoked in intrinsic and extrinsic hand muscles. Mapping with HF-DES-Rest was clinically relevant to identify the cortical site over the primary motor cortex (M1), from which the corticospinal tract can be continuously monitored (and preserved) during tumour resection (intraoperative MEPs monitoring, see Bello et al. 2014). HF-DES was delivered through a constant current monopolar stimulator (straight tip, 1.5 mm diameter (Inomed), with reference/ground on the skull overlying the central sulcus). Depending on the clinical context, either 1 pulse or a train of 5 pulses of constant anodal current pulses (pulse duration 0.5 ms; interstimulus interval, ISI: 3-4 ms) were delivered.

2) <u>Low Frequency Bipolar Stimulation during the hand manipulation task (LF-DES-HMt).</u> LF-DES consisted of trains, lasting 2 to 5 seconds, of biphasic square wave pulses (0.5 ms each phase) at 60 Hz (ISI 16.6 ms) delivered by a constant current stimulator (OSIRIS-NeuroStimulator) integrated into the ISIS-System through a bipolar probe (2 ball tips, 2 mm diameter, separation 5 mm). LF-DES-HMt was delivered mainly on the rostral sector of the hand-knob. In the patients included in this study, the caudal sector of the hand-knob was indeed generally easily excitable and thus identified with HF-DES-Rest, rarely requiring a further investigation with LF-DES-HMt. Due to the small sample of stimulations with LF-DES-HMt, the caudal sites (about <10% of total) were thus not included in the analysis, but they have been discussed according to rostral stimulations and the neurosurgical literature. The LF-DES-HMt was clinically relevant to identify the functional cortical and subcortical frontal boundaries of the resections. To identify cortical and subcortical structures of the rostral hand-knob that had to be preserved, the effect of DES stimulation during HMt execution was assessed (Rossi et al. 2018). This effect of DES was evaluated based on the observation of the movement of the hand and classified as "behavioural outcome". Moreover, the qualitative analysis of the corresponding EMG pattern was used to confirm/clarify the effect of DES on the upper-limb effectors (proximal or distal) evaluated based on movement observation.

The definition of "High Frequency" vs "Low Frequency" paradigms, described in details in a previous study of our group (see Bello et al. 2014), was determined purely by the frequency of shocks within the stimulating train based on the inter stimulus interval (ISI) between two subsequent pulses (3-4 ms for the HF-DES and 16.6 ms for the LF-DES), irrespectively of the number of pulses and train duration.

More detailed description of the surgical procedure, and of the standard intraoperative neurophysiological monitoring and mapping protocol is reported in the Supplementary Material.

2.1 Patients selection. 17 patients (15 right-handed and 2 left-handed) with a glioma affecting the right hemisphere were enrolled. Detailed information on these patients is shown in Table 1. In all patients, the precentral gyrus was exposed for surgical reasons and accessible for DES. Patients included in this study were not enrolled a priori but they were selected after the surgery only when meeting the criteria for the study, i.e. if the clinical procedure, requiring the combination of HF-DES-Rest and LF-DES-HMt for the localization of the safe entry point and of the cortical and subcortical functional boundaries, allowed the investigation of the hand-knob area providing data for the Data Analysis. At present, despite procedures having been performed on both left and right hemisphere lesions, the sample of data that allowed for a significant analysis was collected from patients with right hemisphere lesions, thus we focused on this population.

We ensured that in selected patients the tumours were not infiltrating the regions of interest, i.e. the entire precentral gyrus (specifically the hand-knob region giving rise to the U-shaped connections with the adjacent gyri), the postcentral gyrus, and the posterior limb of the internal capsule and cerebral peduncle hosting the corticospinal fibres (see Supplementary Material, Fig. 5). Each patient underwent preoperative baseline magnetic resonance (MR) studies. Volumetric scan analysis was used to define tumour location and volume. Tumour volume was computed on volumetric fluid-attenuated inversion recovery (FLAIR) MRI scans for low-grade gliomas (LGGs) and on postcontrast T1-weighted MRI scans for high-grade gliomas (HGGs). The minimum distance between the most anterior or the most posterior border of the tumour with respect to the central or the precentral sulcus was determined using Brainlab software. For all the patients included in the study, the distance between these landmarks was ≥ 10 mm (Quiñones-Hinojosa et al. 2003; Fornia et al. 2016).

Patients with sensory-motor deficits and/or cognitive deficits affecting the motor and/or language function were not included in the study. Only patients without seizures, or with a short seizure history well-controlled by one AED were included. All patients gave written informed consent to the surgical and mapping procedure, which followed the principles outlined in "World Medical Association

Table 1.

Patient	Age range	hand dominance	Neurological	Neuro-Psycho_apraxia Bucco-facial	Neuro-Psycho_apraxia ideomotor	lesion side	lesion site	WHO grade	Anesthesia	HF-DES-Rest	LF-DES-HMt	Diffusion-Tractography
1	50-55	Right	Normal	Normal	Normal	Right	Frontal	AstroIII	A-A	X		
2	50-55	Right	Normal	Normal	Normal	Right	Frontoparietal	Other*	A-A	X		
3	30-35	Left	Normal	Normal	Normal	Right	Frontal	OligoIII	A-A	X		
4	40-45	Right	Normal	Normal	Normal	Right	Frontal	AstroIII	A-A	X	X	
5	35-40	Right	Normal	Normal	Normal	Right	Frontal	OligoII	A-A	X	X	X
6	60-65	Right	Normal	Normal	Normal	Right	Frontal	AstroIII	A-A	X	X	X
7	30-35	Right	Normal	Normal	Normal	Right	Frontal	OligoII	A-A	X	X	
8	25-30	Right	Normal	Normal	Normal	Right	Frontal	AstroII	A-A	X		X
9	25-30	Left	Normal	Normal	Normal	Right	Frontal	OligoIII	A-A	X	X	X
10	30-35	Right	Normal	Normal	Normal	Right	Parietal	OligoIII	A-A	X	X	X
11	30-35	Right	Normal	Normal	Normal	Right	Frontal	AstroIII	A-A	X	X	
12	15-20	Right	Normal	Normal	Normal	Right	Frontal	Other*	A-A		X	
13	55-60	Right	Normal	Normal	Normal	Right	Frontoparietal	AstroIII	A-A		X	
14	45-50	Right	Normal	Normal	Normal	Right	Frontotemporal	GBMIV	A-A	X	X	
15	20-25	Right	Normal	Normal	Normal	Right	Frontal	Other*	A-A	X	X	
16	60-65	Right	Normal	Normal	Normal	Right	Frontal	AstroIII	A-A		X	
17	40-45	Right	Normal	Normal	Normal	Right	Frontal	OligoII	A-A		X	X

*Other: 1 inflammatory lesion (patient 2),1 cystic lesion (patient 12) and 1 cortical dysplasia (patient 15).

A-A = Asleep – Awake anaesthesia.

2.2 Hand-Manipulation Task (HMt). LF-DES was applied while patients performed the hand-manipulation task with a specific tool made for this purpose (Rossi et al. 2018; see also Fig. 2C and Supplementary Material). The tool's rectangular base was kept stable close to the patient's hand along the armrest of the operating table, while the patient grasped, hold, rotated and released the cylindrical handle with the thumb and the index finger, likely resembling a precision grip rhythmically

performed. Proximity between the hand and the cylindrical handle allowed the patients to perform the movement using just the fingers, avoiding a possible reaching movement. Each patient, opportunely trained one day before surgery, was asked to perform the task continuously, following an internal generated rhythm without any external cue to instruct the phases of movement nor visual information about the hand or the cylindrical handle movement (i.e. the movement was "haptically driven"). During HMt execution, neuropsychologists performed a real-time monitoring of the patients' behavioural outcome, reporting to the surgeons any arrest, decrease of performance and/or any somatic sensation. During its execution up to 24 muscles were simultaneously recorded including bilateral upper body, lower body and oro-facial muscles. The hand-object interaction during the task execution was video-recorded and synchronized off-line with the EMG signals. At the beginning of the HMt session, 10 seconds (in some cases even longer) of baseline movement (without stimulation) was required to reach stable task execution. When good stability was reached (as assessed based on behavioural outcome and ongoing EMG activity real time monitoring), the surgeon started the stimulation of the investigated areas randomly during task performance. An interval of 3-4 seconds among different stimulation and among different sites was observed to avoid dragging-effects. The effect of the LF-DES-HMt was assessed by means of online and offline observation (behavioural outcome) and confirmed by qualitative EMG-pattern inspection.

2.3 Definition and anatomical localization of the stimulation sites: All the stimulation sites were chosen based on the morphology of the hand-knob according to the surgical flap and based on the margins of the resection planned. Both anatomical localization and the number of the stimulation sites were constrained by the surgical procedure. No additional sites others than those required for clinical needs were added to the brain mapping procedure. Intraoperatively, the central sulcus and the precentral sulcus were chosen as anatomical landmarks for identifying respectively the caudal and rostral sector of the hand-knob region. The procedure requires, first, identification with HF-DES of the site eliciting a motor output with lowest current threshold; above this site the surgeon places a 4-contact subdural strip electrode delivering "train-of-five" pulses to elicit MEPs in a sample of contralateral muscles (see Supplementary Materials; Bello et al. 2014). The localization of this site is always close to the central sulcus according to the extensive surgical experience (L.B. and M.R.) as supported also by results of the present work (see Results). For resection of tumours affecting patients considered for this study, the surgeon, moving anterior along the rostro-caudal line, applied HF-DES also close to the precentral sulcus with the aim of identifying the safe cortical entry point and the border of the resection. Considering that, with respect to the motor output obtained by stimulation of the caudal site (see Results), the motor output of the rostral sector was significantly lower in

amplitude, the rostral region was also tested during the Hand-Manipulation task delivering LF-DES to establish its implication in action execution despite its lower excitability at rest. In this cohort of patients, the caudal region was rarely stimulated with LF-DES, thus the definition of the rostral sites was, at the single subject level, relative to the caudal site as identified with HF-DES (i.e. rostral site = localized anterior and approximately at same medio-lateral of the caudal site, defined based on the proximity to the central sulcus) and verified using the precentral sulcus as anatomical reference. In four patients (P 12, 13, 16, 17, see Table 1) the caudal site was identified with HF-DES, and following this, the rostral sector was stimulated mainly/only with LF-DES to assess the posterior border of the resection. In these cases, the HF-DES data was not included because the number of trials (MEPs) was not adequate for statistical comparison or because the rostral site was investigated only with LF-DES.

2.4 Diffusion Tractography. Diffusion imaging tractography was performed in a subset of six patients (Table 1). Data was acquired on a 3T Siemens Magnetom Verio scanner with an 8 channel head coil, using a HARDI-optimised diffusion weighted single-shot echo-planar sequence along 73 directions with a b-value of 2000s/mm^2 (TE:96ms, TR 10.4ms). Seven interleaved non-diffusion weighted volumes were acquired. The sequence had a matrix size of 128 x 128 x 64 with 2mm isotropic voxels.

2.5 DATA ANALYSIS

2.5.1 Analysis of MEPs (*HF-DES-Rest*). Raw electromyography (EMG) of hand/forearm muscles was recorded with specific software (ISIS, INOMED, sampling rate 20 kHz, notch filter at 50 Hz). For each patient, the raw data, i.e. all the Motor Evoked Potentials (MEPs) recorded during the procedure, were extracted from the acquisition system and resampled at 4 kHz and analysed offline by means of dedicated MATLAB software. For each trial, a window of interest of 100 ms from the stimulus onset was defined. The average background EMG activity and its SD (±1 SD) were then calculated from the last 25 ms of the record (i.e., from 75 to 100 ms). A MEP was considered reliable only when the EMG voltage signal-exceeded the average background ±1 SD (Fornia et al. 2016). All the MEPs were stored based on the location of the stimulating site within the hand-knob sectors (caudal vs rostral). We focused our analysis on the most represented forearm-hand muscles in the data sample (i.e. Extensor Digitorum Communis, EDC; First Dorsal Interosseous, FDI; Abductor Pollicis Brevis, APB; Abductor Digiti Minimi, ADM and Flexor Carpi Radialis, FCR). We considered only MEPs evoked when patients were fully awake and lying with all body parts at rest, avoiding any "facilitation" effect (i.e. increase of excitability) due to unforeseen upper limb

movements. To this end, we visually inspected the raw EMG activity to qualitatively evaluate the background activity at rest. MEPs facilitated by unforeseen muscle contraction were detected and excluded from further analysis.

The main parameter considered for the comparison between caudal and rostral hand-knob was the "cortical excitability" measured with a quantitative analysis aimed at comparing the occurrence and the amplitude of MEPs elicited in the rostral sectors with respect to the caudal ones by stimulating both sectors with the same paradigm, i.e. with the same combination of number of pulses and intensity delivered with HF-DES. To this end, two main parameters were selected to assess differences in cortical excitability between the two sectors:

1) the Caudal Motor Threshold (cMT), defined as the minimum number of pulses (given a fixed intensity of current) and intensity of stimulation (given a fixed number of pulses) required to evoke MEPs in the caudal sector, supposed to be the most excitable based on surgeon's extensive intraoperative experience (L.B., M.R.). For all the procedures that required stimulation of the rostral region with the cMT identified on the caudal region, an offline analysis was performed to verify, within the same patient, if the cMT parameters of stimulations were effective to evoke MEPs in the rostral region.

2) The amplitude of MEPs evoked in the same patients in both the rostral and caudal sectors with the same stimulation parameters (i.e. number of pulses and intensity) was compared.

2.5.2 Behavioural outcome classification (*LF-DES-HMt*). The effect of DES delivered on the rostral hand knob subsector during the HMt (LF-DES-HMt), was evaluated by trained neuropsychologists and neurophysiologists blinded to the stimulation sites by means of an off-line inspection of the video-recorded task performance during surgery of each patient. DES during HMt execution resulted in different effects on the execution, enabling a classification into distinct "behavioural outcomes". Moreover, each identified outcome was also confirmed by visual inspection of the associated muscle pattern (EMG).

2.5.3 Reconstruction of stimulation sites. During the surgery, the brain mapping technique was videotaped and MRI coordinates of all the stimulated sites were acquired by the neuronavigation system. The reconstruction of the exact position of all sites was then computed for each patient with the following procedure. The cortical surface extraction and surface volume registration was computed using the T1 with or without contrast according to the sequence loaded into the neuronavigation system during surgery, by means of Freesurfer software (Fischl 2008). Subsequently the results were loaded onto Brainstorm (a MATLAB toolbox; Tadel et al. 2011), an open source software downloadable under the GNU general public license. The exact position of all the sites was

marked as a scout on the patient's 3D MRI with the aid of Brainstorm. Subsequently, using the same software, each patient's 3D MRI with the respective labelled scouts were co-registered in the MNI space (Ashburner & Friston, 2005). Finally, all the stimulation sites were plotted on the FSAverage template to create a 3D reconstruction of the (right) stimulated hemisphere.

The colour code in Fig. 1 and Fig. 2 reflects the localization of all the stimulation sites during HF-DES-Rest (Fig. 1 A-B) and the classification of the behavioural outcome during LF-DES-HMt (Fig. 2 A-B).

2.5.4 Diffusion tractography. We corrected the diffusion MRI collected in the six patients for head motion, eddy current distortion and susceptibility artefacts using ExploreDTI (Leemans et al. 2009). This data was then processed for both whole brain diffusion tensor and spherical deconvolution tractography, using StarTrack software (www.mr-startrack.com; Dell'Acqua et al. 2010). For spherical deconvolution modelling, a damped Richardson-Lucy algorithm was used with a fibre response parameter of 1.5, 200 iterations, and threshold and geometrical regularisation parameters of 0.04 and 15 respectively (Dell'Acqua et al. 2012). An absolute threshold of 0.0038 was used to exclude spurious local maxima. For both tensor and HARDI models, Euler integration was used for streamline reconstruction, using an angle threshold of 45 and a step-size of 1 (with tensor FA threshold of 0.12). Tractography dissections were performed using a region-of-interest approach by an experienced dissector (H.H.). The corticospinal (corticofugal) projection tracts were dissected using the methods detailed in Catani & Thiebaut de Schotten (2012) and Howells et al. (2018). One inclusion ROI was composed of the entire precentral gyrus, and a second inclusion ROI was used in the brain stem, below the cerebellar peduncles, to constrain the resulting streamlines to display those descending to the brain stem. The U-shaped connections between the precentral gyrus, superior and middle frontal gyrus, and precentral to postcentral gyri were dissected according to Catani et al. (2012). The entire precentral, postcentral, superior frontal and middle frontal gyri were delineated and used as inclusion ROIs for the relevant tracts in all six patients.

2.5.5 Statistical analysis. Statistical analysis was performed only on HF-DES-Rest data acquired by stimulation of both the rostral and the caudal hand-knob sector and was aimed at assessing differences in cortical excitability between the two subsectors in the forearm-hand muscles (EDC, APB, FDI, ADM and FCR). To this end, MEP amplitude evoked by stimulation of the two sectors of the hand-knob, with the same number of pulses and intensity of stimulation, was compared in each single patient. We included in the analysis only muscles responsive to at least five HF-DES-Rest trials in both areas. All the MEPs evoked in the different muscles of the forearm and hand were grouped by

sector (caudal or rostral hand-knob). All MEPs amplitude values were standardized within the area and between muscles (z-score). Mann-Whitney U tests were used to assess statistical differences between the MEP amplitude elicited in the two different hand-knob subsectors.

3. RESULTS

Seventeen patients submitted to awake surgery of a tumour in the right hemisphere, were enrolled in this study. These patients were operated according to functional boundaries by means of the brain mapping technique and Direct Electrical Stimulation (DES). All patients satisfied the required inclusion criteria.

3.1 *HF-DES-Rest*. In 13 patients out of 17 brain mapping was performed with this technique (see Table 1). 30 stimulation sites were recorded, n=14 in caudal-hand-knob (patient mean 1.1, SD 0.3) and n=16 in rostral-hand-knob (patient mean 1.2, sd 0.6) (Fig. 1A). Analysis of the excitability of the two subsectors was performed as follows: 1) in a sample of 5 patients the comparison was based on MEP occurrence in the rostral subsector by applying the same stimulation parameters (number of pulses and intensity of stimulation) defined for the caudal motor threshold (cMT); 2) in 8 patients, where cMT stimulation was not applied on the rostral sector, we analysed the amplitude of MEPs elicited with an over-threshold stimulation delivered on the two subsectors with the same intensity and number of pulses.

1) Analysis of the cMT. According to the clinical procedure, the caudal sector was explored with HF-DES-Rest first and the cMT was defined as the minimum number of pulses and intensity of stimulation required to evoke MEPs in the caudal sector (mean intensity = 5.8mA; mean number of pulses = 5). In 5 out of 13 patients, HF-DES was applied at the cMT also on rostral hand-knob. In all patients stimulation at cMT was effective in eliciting reliable MEPs in the caudal sector in the entire sample of muscles analysed (APB, FDI, EDC, ADM, FCR), while when applied on the rostral sector it systematically failed to evoke reliable MEPs that were clearly distinguishable from EMG background activity (see Methods) in the entire sample of muscles (Fig. 1C). This data suggests a non-homogeneous distribution of excitability in the two subsectors, with the caudal one more excitable than the rostral.

2) Analysis of the MEP amplitude. Given that, due to clinical constraints, direct comparison of the effect of stimulation at cMT over the two subsectors was not performed in 8 out of 13 patients, an alternative analysis was considered to assess the excitability of the hand-knob in the rostro-caudal direction. In this cohort of patients, the surgeon used an over-threshold stimulation protocol to induce

MEPs on both sides, thus it was possible to compare MEP amplitude evoked with same stimulation parameters in the two subsectors. As a first observation, DES stimulation of the caudal hand-knob elicited reliable MEPs in all the analysed hand muscles, while when delivered on the rostral hand-knob with the same stimulation parameters (number of pulses and intensity) DES elicited MEPs only in some of the analysed hand muscles. Due to this condition, comparison of MEP amplitude using the same DES parameters in the two subsectors was allowed only in the muscles in which the over-threshold stimulation elicited reliable MEPs in both subsectors. This meant that different combinations of muscles were compared in each patient: 2 out of 5 muscles (EDC; FDI) in Patient 5; 1 out of 5 (FCR) in Patient 6; 1 out of 5 (APB) in Patient 7; 3 out of 5 (ADM; FDI; APB) in Patient 8; 1 out of 5 (FDI) in Patient 9; 1 out of 5 (APB) in Patient 10; 2 out of 5 (EDC; APB) in Patient 11; 3 out of 5 (EDC; ADM; FDI) in Patient 15. For all patients that underwent this analysis, MEP amplitudes evoked by HF-DES delivered on rostral hand-knob were significantly lower compared with MEP amplitudes evoked by HF-DES delivered on caudal hand-knob (Patient 5 U=0, p=0.000006; Patient 6 U=0, p=0.000311; Patient 7 U=0, p=0.002165; Patient 8 U=21, p=0.000012; Patient 9 U=0, p=0.000074; Patient 10 U=0, p=0.007937; Patient 11 U=0, p=0.000666; Patient 15 U=7, p=0.0000000003 (Fig. 1D). Although the number of muscles were not the same in all patients, a statistically significant difference in amplitude was observed in each patient, which strongly supports the results obtained with cMT. Figure 3A shows all the stimulation sites plotted on the 3D MNI brain reconstruction of Patient 7 (1) and the MEP average of 10 trials from the caudal and rostral hand-knob in the same patient (2).

3.2 *LF-DES-HMt.* This condition was analysed in 13 patients out of 17 (see Table 1). The behavioural outcome occurring during LF-DES stimulation while patients were performing the HMt was assessed in 20 sites on the rostral hand-knob (patient mean 1.54, sd 1) (Fig. 2A). Offline visual inspection of the hand-object interaction during, and in absence, of DES lead to classification of two "anomalous" hand/arm behavioural outcomes induced by DES:

- **Dysfunctional Hand Movement (dHM)** (10 sites out of 20 (50%), Fig. 2A)**:** during DES, HMt was impaired due to the occurrence of hand movement clearly dysfunctional (dHM) for the achievement of the task. Precisely two possible involuntary configurations of the hand induced by stimulation were observed: -closure/contraction of the hand/fingers (see Video 1, Supplementary Materials); -progressive aperture of the hand, sometimes coupled with clonic-like twitches (see Video 2, Supplementary Materials). Recruitment of distal muscles not required to perform the HMt was observed by inspection of EMG recording. In 5 of 10 sites, the involuntary recruitment involved also the forearm and/or proximal muscles.

421   -   **Suppression of Hand Movement (sHM)** (10 sites out of 20 (50%), Fig. 2A): during DES the

422   HMt was impaired due to an arrest of hand and finger movement (sHM) (see Video 3,

423   Supplementary Materials). In 5 out of 10 sites the loss of postural hand tone was coupled with

424   a clear activation of the forearm/proximal muscles leading to a flexion or an extension of the

425   arm (see Video 4, Supplementary Materials).

426   Overall a significant impairment in HMt execution correlated with DES stimulation, although with

427   different features. In dHM sites, DES impaired the task by inducing an accessory activation of hand

428   and arm muscles, producing a dysfunctional hand-object interaction. In sHM sites, DES impaired the

429   task by inhibiting ongoing activation of the muscles required for the movement. Both interference

430   effects could be elicited in different sites in the same patient (Figure 3B). In order to investigate if the

431   observed outcomes were task-dependent responses rather than being the result of the involuntary

432   progressive recruitment of all the muscles represented in the stimulated area, irrespective to their

433   reciprocal action (e.g. agonist and antagonists) in the ongoing task, we analysed data in 4 patients

434   stimulated, for clinical reasons, with LF-DES at rostral sites in different conditions that we can

435   consider as "control". In 3 patients, 3 sites classified as sHM and 1 site classified as dHM, were also

436   stimulated while patient's hand was at rest and failed to show upper-limb movement and/or EMG

437   activation in proximal and distal upper limb muscles. In 1 patient, a site classified as sHM, was

438   stimulated while the patient was asked to open and close the hand: no interference on movement

439   neither activation of distal and/or proximal muscle was observed. Interestingly the same site, when

440   stimulated during HMt arrested the hand movement and activates the biceps.

441   The results obtained from controls showed that DES in the same sites positive for the HMt did not

442   evoke any significant electrophysiological and behavioral response at rest or when performing a

443   simple opening and closing of the hand. This indicates that the execution of the task significantly

444   changes the excitability of the rostral sites, leading to the described outcome. Overall, these results

445   support the hypothesis that sHM and dHM are task-dependent outcomes.

446   Finally, when delivered on the caudal hand-knob, LF-DES always resulted in a recruitment of hand-

447   arm muscles both during the HMt and in the resting condition.

448

449   **3.3 Tractography.** In six patients, the corticofugal and U-shaped tracts were traced between the

450   precentral gyrus and the superior frontal and middle frontal gyrus (see Fig. 4). Additionally, the tracts

451   connecting the precentral and postcentral gyrus were also traced. The main finding was that the tracts

452   connecting dorsal premotor regions with the precentral gyrus terminate solely within the rostral

453   portion of M1 (rostral hand-knob) and were distinct from tracts connecting the precentral gyrus with

454   the postcentral gyrus, that terminated in the caudal portion of M1 (caudal hand-knob). These

terminations corresponded with the same sectors previously identified by DES as sectors that had different cortical excitability, the caudal showing higher excitability and preferentially connected with the postcentral gyrus, while the rostral sites showed lower excitability and preferentially connected with the dPM area (Fig. 4). The corticofugal projections extended equally into both caudal and rostral sectors of the precentral gyrus, when using the diffusion tensor (Fig. 4) and spherical deconvolution for modelling the tracts.

4. DISCUSSION

The aim of the study was to investigate whether the human hand-knob region of precentral gyrus can be considered, in the rostro-caudal direction, a unitary cortical area or rather if it could be subdivided in different anatomo-functional subsectors, as suggested by studies in the monkey (Rathelot & Strick, 2008; Witham et al. 2016). Our results suggest a subdivision of the human hand-knob in a rostral and caudal sector, based on the observed difference in functional properties and patterns of connectivity.

4.1 Cortical excitability within the hand-knob. A direct comparison of cortical excitability in the caudal and rostral hand-knob was performed based on a comparison of the motor output of the two subsectors elicited by HF-DES-Rest. Given the clinical constraints, cortical excitability was here investigated with a complementary approach. On one side, the two sectors were compared with respect to stimulation threshold: rostral and caudal sectors were stimulated with the parameters of stimulation necessary to evoke MEPs when delivered over the caudal sector (the Caudal Motor Threshold, cMT) used as reference. Should the two sectors be equally excitable, the cMT would be expected to elicit comparable responses in both sectors. The alternative approach we used, in patients for whom this type of comparison could not be performed, involved comparing the MEP amplitudes themselves, elicited in the two sectors with the same number of pulses and stimulation intensity. Again, should the two sectors be equally excitable, the amplitude would not be different. These two approaches for assessing differences in cortical excitability suggest that a non-homogeneous rostro-caudal distribution of cortical excitability exists within the hand-knob. The caudal sector showed significantly higher excitability with respect to the rostral one. This result may also be supported by the pattern of muscles activated by the over-threshold stimulations in the two sectors: the same stimulation protocol induced activation of a higher number of muscles when applied to the caudal sector compared with the rostral (a mean of 5 muscles per patient in the caudal hand-knob and a mean of 1.6 muscle per patient in the rostral hand-knob). This latter observation, although interesting, is not conclusive and future studies are required to clarify whether this might be due to different

organization of muscle synergies in the two cortical districts. With regard to a gradient of rostro-caudal excitability, the functional organization of the monkeys' M1 can be used as a benchmark. In the monkey M1, the highest excitability is observed in the caudal sector, the new-M1, which is different with respect to the rostral sector, the old-M1. Rathelot and Strick (2008), using retrograde trans-synaptic transport of rabies virus from the finger, elbow and shoulder muscles, found that the traced corticomotoneuronal (CM) cells correspond only with the low-threshold sites in the new-M1. Evidence of CM connections originating from both old and new-M1 was more recently provided by Witham and colleagues (2016), although confirming different structural patterns of corticospinal connectivity, since from the old-M1 originate slower corticospinal (CST) fibers when compared to the faster new-M1. Based on functional evidence, our hypothesis is that the rostral sector close to the precentral sulcus explored with DES and emerging as the less excitable sector, might correspond to the monkeys' old-M1 located on the crest of the precentral sulcus, while the caudal sector, close to the central sulcus, might correspond to the new-M1 buried in the central sulcus. The functional matching between the human and monkeys hand-knob region suggested by the intraoperative data might let us speculate that the two sectors, in humans, contribute in different proportions to the CST. However, no conclusive interpretation in light of non-human old and new-M1 can be claimed, since we cannot support the neurophysiological data with architectonic investigation of the caudal and rostral sectors in our patients.

Another possible explanation for the excitability gradient observed within the hand-knob deserves discussion. Architectonic data (Geyer et al. 1996) suggests that human M1 is buried on the bank of the central sulcus, where, due to clinical constraints, HF-DES-Rest cannot be directly applied. Should this be the case, DES delivered on caudal convexity proximal to central sulcus may easily reach and excite cortical neurons in the sulcus, while a higher intensity of current would be needed to excite the same neurons, when DES is delivered further away on the convexity close to the precentral sulcus. This would explain the lower motor threshold of the caudal sector, challenging the idea of a functional subdivision of M1 in distinct subsectors. An alternative hypothesis of our results might be grounded on fMRI data in humans, showing a partial overlap of the premotor cortices (PMC) and M1 on the convexity of the PreCG (Mayka et al. 2006; Fan et al. 2016). The cortical parcellation described across several neuroimaging modalities in a large number of healthy subjects supports this data (Glasser et al. 2016). In this light, DES applied on caudal and rostral sector of the precentral gyrus may be stimulating area 4 and 6d respectively, reasonably suggesting that the rostral hand-knob might actually represent a transition area from M1 toward the dorsal premotor cortex (dPM) (Fig. 1B). This hypothesis finds a further support in the anatomo-functional studies investigating the dPM in monkey, particularly focusing on its caudal portion called F2, a specific architectonic area (Matelli et al. 1991)

523 connected with both primary motor cortex and spinal cord (He et al. 1993; Geyer et al. 2000; Dum &

524 Strick 2005) and requiring a higher current intensity when compared to M1 to elicit a motor output

525 (Raos et al. 2003, 2004; Dum & Strick 2005). When compared to M1, F2 shows fewer corticospinal

526 projections (He et al. 1993). This data might suggest that the intraoperative "rostral hand-knob" shares

527 similarities with the caudal F2.

528

529 **4.2 The role of human rostral hand-knob in action execution.** The combined approach used to

530 investigate this area suggests that the rostral sector is strongly involved in the recruitment of adequate

531 muscle activity to perform hand actions. The clear disruption of the intraoperative hand task suggests

532 that, despite its lower excitability at rest (HF-DES-Rest), the rostral hand-knob is highly responsive

533 during LF-DES-HMt, leading to hypothesize its involvement in the neural network controlling action

534 execution. Results from control conditions in 4 patients, in which the stimulation of the same sites

535 positive for the HMt did not evoke any overt behavioural response neither a slightly muscle activation

536 in the proximal and distal muscles of the upper limb, support this hypothesis. However, despite no

537 direct comparison was allowed with the caudal sector, which was not systematically investigated with

538 this technique for clinical reasons (see Methods), the analysis of the specific behavioural outcome

539 occurring during stimulation provided two interesting elements to speculate on the possible role of

540 rostral hand-knob in hand manipulation. First, two different outcomes occurred when DES was

541 applied on the rostral hand-knob during HMt: an involuntary recruitment of the distal muscles

542 (Dysfunctional Hand Movement, see Video 1-2 in the Supplementary Materials), or an arrest of hand

543 and finger movements (Suppression of Hand Movement, see Video 3-4 in the Supplementary

544 Materials). Second, the two responses were not clearly segregated in the rostral hand-knob (Fig. 2A).

545 The two outcomes of DES interference observed, dHM and sHM, were not entirely expected. As part

546 of the primary motor cortex, the stimulation of the rostral hand-knob with LF-DES was expected to

547 arrest the task by eliciting an a-specific recruitment of all the hand-forearm muscles progressively

548 involving distal to proximal muscles by increasing the intensity of stimulation (see Park et al. 2004;

549 Boudrias et al 2010; Bello et al. 2014). Surprisingly, LF-DES interferes with the task either by

550 suppressing the ongoing muscle activity, or by changing the pattern of muscle synergies activated,

551 resulting in a dysfunctional activation. LF-DES applied on the caudal hand-knob, where the hand

552 representation of M1 is supposed to be hosted, evoked a clear progressive muscles recruitment both

553 at rest (Penfield et al. 1937; Bello et al. 2014), involving a number of muscles dependent on the

554 intensity of the stimulation (see Park et al. 2004; Boudrias et al 2010; Bello et al. 2014), and during

555 HMt execution, in line with what has been suggested in the literature (Rech et al. 2016; 2017).

556 However, the response to LF-DES delivered during HMt on the rostral hand-knob (i.e. a suppression

or a selective activation of different patterns of distal and proximal muscle activation leading to dysfunctional movements such as an aperture or a closure of the hand on the handle of the tool) is not coherent with this kind of tetanic and a-specific recruitment. This data points to the rostral hand-knob as an area involved in shaping the motor output rather than in hosting the muscle representations used for the transmission of the motor command to the spinal motoneurons.

Interestingly, both the behavioural outcomes (50% of dHM and 50% of sHM) were coupled with forearm and/or proximal muscle accessory recruitment leading to an unrequired arm movement (i.e flexion or extension) (see Fig. 3B 1-2 for a single subject example and Video 1 and 4 in the Supplementary Materials). Monkey studies report a muscle-based map of M1 in which a central core of distal muscles (buried in the central sulcus) is surrounded by an intermediate zone of overlapped distal and proximal muscles and by a *horseshoe-shaped* proximal muscle zone (Park et al 2001; Hudson et al. 2017). Coherently, high-resolution fMRI (Meier et al. 2008) confirmed in humans a core of digit representation in the PreCG bracketed by a wrist and forearm area. The occurrence of dHM and sHM in the rostral sector may indicate a role of the rostral hand-knob in the implementation of functional synergies between distal and proximal muscles during upper-limb multi-joint movement. A focused analysis is mandatory to address this issue, however the similarities suggested above between the rostral sector of the human hand-knob and the non-human dPM, particularly area F2, seems coherent with proximal muscle involvement. In monkeys, F2 neurons are active during reaching and grasping movements (Kalaska et al. 1997; Cisek et al 2003; Nelissen et al. 2017) and their discharge correlates with relevant features of goal-related actions (Raos et al. 2004). Coherently, F2 has a mixed proximal and distal representation (Dum & Strick, 2005; Boudrias et al 2010). In humans, rTMS applied to dPM affects hand movement by decoupling the holding phase of grasping with the lifting phase requiring proximal muscles to achieve the goal (Davare et al. 2006). A recent meta-analytic connectivity model based on co-activation patterns across active tasks (MACM-CBP) in humans (Genon et al. 2017) described rostro-caudal organization of the right dPM, confirming the involvement of the caudal sector, adjacent to M1, in action execution. The effect of DES on HMt suggests the rostral hand-knob as a transition zone between M1 and dPM (Fig. 2B).

From a behavioural perspective, suppression of hand movements (sHM) could recall the outcome described during DES of the so-called *negative motor areas* (NMAs) (Luders er al. 1995). However, some observations inferred from the EMG recording, prevent us from classifying the sHM sites as NMAs. We show that in half of stimulations, "negative motor phenomena" observed as arrest of hand movement was actually coupled with a clear positive motor response, i.e. activation of forearm/proximal muscles promoting movement of the proximal part of the upper-limb. To our knowledge, this mixed effect has not been described in literature and, reasonably, this cannot be

defined as a "negative" phenomenon when considered as a whole. Moreover, historically the anatomical localization of NMAs is reported to occur mainly in the SMA complex and the inferior frontal gyrus (Filevich et al. 2012). Although some studies report that negative motor responses can be evoked in the hand-knob sector (Nii et al. 1996; Enatsu et al. 2013), none of them have validated the behavioural outcome with simultaneous EMG activity recorded in the movers to assess whether the observed negative effect, i.e. the "arrest" of the ongoing movement, was due to recruitment or suppression of muscle phenomena. Our results indicate that, despite the largely accepted criteria for selecting negative motor responses based on observation of the overt component of an action, behavioural data coupled with EMG recording produces a different categorization of DES-outcome. The arrest of the hand/finger coupled with forearm/proximal recruitment, for instance, could be the result of a dysfunctional re-shaping of muscles synergies required by the HMt, instead of a positive process of distal muscle inhibition. In some cases, it could not be detected without EMG recording of muscles not directly involved in the ongoing task. Further, we showed both "negative" and "positive" responses in the same sector without clear segregation, the latter consisting in dysfunctional movements with task-unrelated EMG recruitment. However, no conclusions can be discussed in the absence of more detailed studies aimed at analysing this issue.

The overlapping of dHM and sHM on the rostral sector deserves a specific methodological comment. In the intraoperative setting, the delivery of LF-DES during HMt was randomly applied during the task and was not triggered during a specific phase of the task execution (e.g. the 'shape', 'hold', 'rotate' or 'release' phases) which involve different muscles synergies. In such a context, we cannot exclude that the occurrence of different excitatory (dHM) and inhibitory (sHM) effects regarding the distal muscles by stimulating the same rostral sector, might be a HMt phase-dependent phenomenon rather than a specific cortical site-related effect.

4.3 HF-DES-Rest and LF-DES-HMt in relation to white matter connectivity of the human hand-knob.

We performed virtual dissections of the tracts extending from the hand-knob region using diffusion imaging in a subset of six patients, specifically the local connections between the hand-knob and superior and middle frontal regions, and those with the postcentral gyrus, as well as long-range corticofugal projection tracts extending to the brainstem. We aimed at evaluating whether the functional differences detected between the rostral and caudal sectors corresponded with different patterns of connectivity. Differences between the two sectors emerged when considering the cortico-cortical connections only.

Corticofugal tracts were identified, but we could not detect specific terminations in either the rostral or caudal sector. However, a gradient in laminar structure of the hand-knob region has previously been reported based on histological and ex-vivo diffusion imaging, suggesting a different corticospinal composition in rostro-caudal direction (Geyer et al. 1996, Bastiani et al. 2016). Evaluating rostro-caudal differences in projection tracts requires a higher spatial resolution, however we used a voxel size of 2mm voxel, which may contain up to 5 million axons (Walhovd et al. 2014). This lack of sensitivity therefore prevents us from distinguishing between actual corticospinal fibres and alternative corticofugal tracts that may terminate in subcortical structures. For this reason, at present is not possible to disclose the existence of microstructural differences within the bundle of corticospinal fibres projecting from the two sectors of the hand-knob region as suggested by the intraoperative data analysis. Further, diffusion tractography shows a lower density of corticospinal fibres exists in the right hemisphere (Catani & Thiebaut de Schotten, 2008; Howells et al. 2018), thus future studies are mandatory to investigate whether rostro-caudal variation of corticospinal tracts exists within the left hemisphere.

Regarding the cortico-cortical connections, we examined the local white matter connectivity in this region, described as taking a 'poppy flower'-like formation (Figure 4A right panel, Catani et al. 2012). The frontal U-shaped tracts projected between the superior and middle frontal gyrus and the rostral but not caudal sector of the hand-knob, whereas the fronto-parietal tracts connected the postcentral gyrus and the caudal sector exclusively (Figure 4). Although differences in local connectivity of M1 have not yet been reported in the Old World monkey, a similar distinction between rostral intrafrontal and caudal fronto-parietal connections has been described in owl and squirrel monkeys (Stepniewska et al. 1993, 2006; Dea et al. 2016), suggesting a dedicated analysis is required to substantiate this observation of connectional patterns in a higher number of subjects.

The observed differences in local connectivity may reflect the functional role that each sector plays in control of the hand. Our results show that LF-DES-HMt on the rostral crown of the hand region of the precentral gyrus interrupts task performance. In the six subjects with diffusion tractography and corresponding intraoperative stimulation sites, this region corresponded with the intrafrontal tracts. The cortical regions connected by these U-shaped tracts (the rostral hand-knob region and anterior premotor areas), are suggested to play a role in mediating motor planning and execution (Catani et al. 2012). When matching the observed patterns of white matter connectivity with intraoperative neurophysiological data, the hypothesis of the rostral region as a caudal extension of the dorsal premotor cortex involved in motor programming of upper-limb movement seems more reasonable. Whether the precentral-postcentral connections play a similar role, or are more involved in ongoing

659 tactile and somatosensory feedback in the executive stage of movement execution, remains to be
660 investigated.
661

662 **4.4 Limitations**: The main result of the study, based on the quantitative analysis of the motor output
663 elicited with HF-DES-Rest, shows a non-homogeneous rostro-caudal distribution of cortical
664 excitability, with the caudal hand-knob being the most excitable sector. Although we show
665 consistency in this result across the patients studied, some limitations should be considered.
666 Concerning the hemisphere investigated, the pattern of cortical excitability of the hand-knob region
667 must be verified also in the left hemisphere, particularly when considering the left-lateralization of
668 the corticospinal tract (Catani et al. 2011; Catani & Thiebaut de Schotten 2012; Howells et al. 2018).
669 Moreover, due to clinical constraints, the central sulcus cannot be unfolded preventing a direct
670 investigation of the cortex localized on its anterior bank, an area that, from architectonic studies,
671 might suggest the presence of the highest concentration of corticomotoneuronal cells (Geyer et al.
672 1996). The effect of LF-DES during the Hand Manipulation task was assessed by means of a
673 behavioural classification based on the inspection, blinded to the stimulation sites, of the videotaped
674 task disruptions aligned with EMG recording. A more objective classification would benefit this type
675 of study, such as one computer-based and subject-independent, however the first authors (L.V and
676 L.F) used strict behavioural criteria blind from stimulated sites to overcome this limitation. Both HF-
677 DES-Rest and LF-DES-HMt results must be confirmed in a wider sample of subject and stimulations.
678 The intraoperative brain mapping paradigm is accomplished according only to tumour resection
679 planned by means of functional boundaries. The location of the brain tumours is variable in different
680 individuals, thus it is difficult to enrol suitable subjects and acquire high numbers of stimulation sites
681 to improve power when examining brain activity for research purposes. The existence of different
682 patterns of short-range cortico-cortical U-shaped connections according to rostro-caudal directions
683 must be considered a preliminary result, given the low number of patients with HARDI acquisition.
684 Investigating these functions in non-neurotypical brain tissue has potential limitations, considering
685 the possible reorganization of function with respect to the healthy brain (especially for low-grade
686 gliomas). To account for this, we applied strict inclusion criteria for each patient in order to avoid
687 possible confounding results. Finally, we believe that the high spatio-temporal resolution, the strong
688 causal relationship between stimulation and behavioural outcome (Mandonnet et al. 2010), and the
689 inclusion criteria adopted by our group contribute to make reliable the results of the present study.
690

691 **4.5 Conclusions.** The present study first investigated the functional organization of the human hand-
692 knob area in the rostro-caudal direction, using a direct electrophysiological approach. A gradient of

cortical excitability along this axis emerges, with the caudal hand-knob being the most excitable sector, based on quantitative analysis of the motor output elicited with HF-DES-Rest. The specific pattern of interference occurring when stimulation was delivered on the rostral hand-knob during a dedicated hand manipulation task, suggests that this sector may represent a crucial area for shaping functional synergies for hand-object interaction. Although the spatial limitations of tractography prevented conclusive interpretation of corticospinal involvement, different patterns of local connectivity between the rostral and caudal sectors with adjacent areas were observed. Overall, our results suggest that the human hand-knob can be subdivided into different functional sectors, which may reflect either the rostro-caudal heterogeneity of monkeys' M1, or the existence of a transitional cortical area between M1 and caudal dorsal premotor cortex.

References

Amiez C, Petrides M. 2018. Functional rostro-caudal gradient in the human posterior lateral frontal cortex. Brain Struct Funct. 223(3):1487-1499.

Ashburner J, Friston KJ. 2005. Unified segmentation. Neuroimage. 26(3):839-51.

Bastiani M, Oros-Peusquens AM, Seehaus A, Brenner D, Möllenhoff K, Celik A, Felder J, Bratzke H, Shah NJ, Galuske R, Goebel R, Roebroeck A. 2016. Automatic Segmentation of human cortical layer-complexes and architectural areas using ex vivo diffusion MRI and its validation. Front Neurosci. 10:487.

Bello L, Acerbi F, Giussani C, Baratta P, Taccone P, Songa V. 2006. Intraoperative language localization in multilingual patients with gliomas. Neurosurgery. 59:115-125.

Bello L, Riva M, Fava E, Ferpozzi V, Castellano A, Raneri F, Pessina F, Bizzi A, Falini A, Cerri G. 2014. Tailoring neurophysiological strategies with clinical context enhances resection and safety and expands indications in gliomas involving motor pathways. Neuro Oncol. 16:1110-1128.

Binkofski F, Fink GR, Geyer S, Buccino G, Gruber O, Shah NJ, Taylor JG, Seitz RJ, Zilles K, Freund HJ. 2002. Neural activity in human primary motor cortex areas 4a and 4p is modulated differentially by attention to action. J Neurophysiol. 88(1):514-9.

Boling W, Olivier A, Bittar RG, Reutens D. 1999. Localization of hand motor activation in Broca's pli de passage moyen. J Neurosurg. 91(6):903-10.

Borra E, Gerbella M, Rozzi S, Luppino G. 2017. The macaque lateral grasping network: a neural substrate for generating purposeful hand actions. Neurosci Biobehav Rev. 75:65-90.

Boudrias MH, McPherson RL, Frost SB, Cheney PD. 2010. Output properties and organization of the forelimb representation of motor areas on the lateral aspect of the hemisphere in rhesus macaques. Cereb Cortex. 20(1):169-86.

Broca P. 1888. Description ele´mentaires des circonvolutions ce´re´brales de l'homme. Me´moires d'Anthropologie. Memo Paris: C. Reinwald. 707–804.

Catani M, Thiebaut de Schotten M. 2008. A diffusion tensor imaging tractography atlas for virtual in vivo dissections. Cortex. 44(8):1105-32.

Thiebaut de Schotten M, Ffytche DH, Bizzi A, Dell'Acqua F, Allin M, Walshe M, Murray R, Williams SC, Murphy DG, Catani M. 2011. Atlasing location, asymmetry and inter-subject variability of white matter tracts in the human brain with MR diffusion tractography. Neuroimage. 54(1):49-59.

Catani M, Thiebaut de Schotten M. 2012. Atlas of human brain connections. Oxford. New York, NY: Oxford University Press.

Catani M, Dell'acqua F, Vergani F, Malik F, Hodge H, Roy P, Valabregue R, Thiebaut de Schotten M. 2012. Short frontal lobe connections of the human brain. Cortex. 48(2):273-91.

Caulo M, Briganti C, Mattei PA, Perfetti B, Ferretti A, Romani GL, Tartaro A, Colosimo C. (2007). New morphologic variants of the hand motor cortex as seen with MR imaging in a large study population. AJNR Am J Neuroradiol. 28(8)1480-5.

Cisek P, Crammond DJ, Kalaska JF. 2003. Neural activity in primary motor and dorsal premotor cortex in reaching tasks with the contralateral versus ipsilateral arm. J Neurophysiol. 89(2):922-42.

Davare M, Andres M, Cosnard G, Thonnard JL, Olivier E. 2006. Dissociating the role of ventral and dorsal premotor cortex in precision grasping. J Neurosci. 26(8):2260-8.

Dea M, Hamadjida A, Elgbeili G, Quessy S, Dancause N. 2016. Different patterns of cortical inputs to subregions of the primary motor cortex hand representation in cebus apella. Cereb Cortex. 26(4):1747-61.

Dell'acqua F, Scifo P, Rizzo G, Catani M, Simmons A, Scotti G, Fazio F. 2010. A modified damped Richardson-Lucy algorithm to reduce isotropic background effects in spherical deconvolution. Neuroimage. 49(2):1446-58.

778 Dell'Acqua F, Simmons A, Williams SC, Catani M. 2012. Can spherical deconvolution provide more

779 information than fiber orientations? Hindrance modulated orientational anisotropy, a true-tract

780 specific index to characterize white matter diffusion. Hum Brain Mapp. 34(10):2464-83.

781

782 Dum RP, Strick PL. 2005. Frontal lobe inputs to the digit representations of the motor areas on the

783 lateral surface of the hemisphere. 9;25(6):1375-86.

784

785 Enatsu R, Matsumoto R, Piao Z, O'Connor T, Horning K, Burgess RC, Bulacio J, Bingaman W, Nair

786 DR. 2013. Cortical negative motor network in comparison with sensorimotor network: a cortico-

787 cortical evoked potential study. Cortex. 49(8):2080-96.

788

789 Fan L, Li H, Zhuo J, Zhang Y, Wang J, Chen L, Yang Z, Chu C, Xie S, Laird AR, Fox PT, Eickhoff

790 SB, Yu C, Jiang T. 2016. The human brainnetome atlas: a new brain atlas based on connectional

791 architecture. Cereb Cortex. 26:3508-3526.

792

793 Filevich E, Kühn S, Haggard P. 2012. Negative motor phenomena in cortical stimulation:

794 implications for inhibitory control of human action. Cortex. 48(10):1251-61.

795

796 Fischl B, Rajendran N, Busa E, Augustinack J, Hinds O, Yeo BT, Mohlberg H, Amunts K, Zilles K.

797 2008. Cortical Folding Patterns and Predicting Cytoarchitecture. Cereb Cortex. 18:1973—1980.

798

799 Fornia L, Ferpozzi V, Montagna M, Rossi M, Riva M, Pessina F, Martinelli Boneschi F, Borroni P,

800 Lemon RN, Bello L, Cerri G. 2016. Functional characterization of the left ventrolateral premotor

801 cortex in humans: a direct electrophysiological approach. Cereb Cortex. 1-17.

802

803 Genon S, Li H, Fan L, Müller VI, Cieslik EC, Hoffstaedter F, Reid AT, Langner R, Grefkes C, Fox

804 PT, Moebus S, Caspers S, Amunts K, Jiang T, Eickhoff SB. 2017. The Right Dorsal Premotor Mosaic:

805 Organization, Functions, and Connectivity. Cereb Cortex. 27(3):2095-2110

806

807 Geyer S, Ledberg A, Schleicher A, Kinomura S, Schormann T, Bürgel U, Klingberg T, Larsson J,

808 Zilles K, Roland PE. 1996. Two different areas within the primary motor cortex of man. Nature.

809 382(6594):805-7.

810

Geyer S, Matelli M, Luppino G, Zilles K. 2000. Functional neuroanatomy of the primate isocortical motor system. Anat Embryol. 202(6):443-74.

Glasser MF, Coalson TS, Robinson EC, Hacker CD, Harwell J, Yacoub E, Ugurbil K, Andersson J, Beckmann CF, Jenkinson M, Smith SM, Van Essen DC. 2016. A multi-modal parcellation of human cerebral cortex. Nature. 536(7615):171-178.

He SQ, Dum RP, Strick PL. 1993. Topographic organization of corticospinal projections from the frontal lobe: motor areas on the lateral surface of the hemisphere. J Neurosci. 133:952–980.

Howells H, Thiebaut de Schotten M, Dell'Acqua F, Beyh A, Zappalà G, Leslie A, Simmons A, Murphy DG, Catani M. 2018. Frontoparietal tracts linked to lateralized hand preference and manual specialization. Cereb Cortex. 28(7):2482-2494.

Hudson HM, Park MC, Belhaj-Saïf A, Cheney PD. 2017. Representation of individual forelimb muscles in primary motor cortex. J Neurophysiol. 118(1):47-63.

Kalaska JF, Scott SH, Cisek P, Sergio LE. 1997. Cortical control of reaching movements. Curr Opin Neurobiol. 7(6):849-59.

Kleinschmidt A, Nitschke MF, Frahm J. 1997. Somatotopy in the human motor cortex hand area. A high-resolution functional MRI study. Eur J Neurosci. 9(10):2178-86.

Leemans A, Jeurissen B, Sijbers J, Jones DK .2009. ExploreDTI: a graphical toolbox for processing, analyzing, and visualizing diffusion MR data. Proc Int Soc Magn Reson Med. 17: 3537.

Lüders HO, Dinner DS, Morris HH, Wyllie E, Comair YG. 1995. Cortical electrical stimulation in humans. The negative motor areas. Adv Neurol. 67:115-29.

Mayka MA, Corcos DM, Leurgans SE, Vaillancourt DE. 2006. Three-dimensional locations and boundaries of motor and premotor cortices as defined by functional brain imaging: a meta-analysis. Neuroimage. 31(4):1453-1474.

Mandonnet E, Winkler PA, Duffau H. 2010. Direct electrical stimulation as an input gate into brain functional networks: principles, advantages and limitations. Acta Neurochir (Wien). 152(2):185-93.

845

846 Matelli M, Luppino G, Rizzolatti G. 1991. Architecture of superior and mesial area 6 and the adjacent
847 cingulate cortex in the macaque monkey. J Comp Neurol. 311(4):445-62.

848

849 Meier JD, Aflalo TN, Kastner S, Graziano MS. 2008. Complex organization of human primary motor
850 cortex: a high-resolution fMRI study. J Neurophysiol. 100(4):1800-12.

851

852 Nelissen K, Fiave PA, Vanduffel W. 2017. Decoding grasping movements from the parieto-frontal
853 reaching circuit in the nonhuman primate. Cereb Cortex. 1-15.

854

855 Nii Y, Uematsu S, Lesser RP, Gordon B. 1996. Does the central sulcus divide motor and sensory
856 functions? Cortical mapping of human hand areas as revealed by electrical stimulation through
857 subdural grid electrodes. Neurology. 46(2):360-7.

858

859 Park MC, Belhaj-Saïf A, Gordon M, Cheney PD. 2001. Consistent features in the forelimb
860 representation of primary motor cortex in rhesus macaques. J Neurosci 21: 2784–2792.

861

862 Park MC, Belhaj-Saïf A, Cheney PD. 2004. Properties of primary motor cortex output to forelimb
863 muscles in rhesus macaques. J Neurophysiol. 92(5):2968-84.

864

865 Penfield W, Boldrey E. 1937. Somatic motor and sensory representation in the cerebral cortex of man
866 as studied by electrical stimulation. Brain. 9:389-443.

867

868 Quiñones-Hinojosa A, Ojemann SG, Sanai N, Dillon WP, Berger MS. 2003. Preoperative correlation
869 of intraoperative cortical mapping with magnetic resonance imaging landmarks to predict localization
870 of the Broca area. J Neurosurg. 99(2):311-8.

871

872 Raos V, Franchi G, Gallese V, Fogassi L. 2003. Somatotopic organization of the lateral part of area
873 F2 (dorsal premotor cortex) of the macaque monkey. J Neurophysiol. 89(3):1503-18.

874

875 Raos V, Umiltá MA, Gallese V, Fogassi L. 2004. Functional properties of grasping-related neurons
876 in the dorsal premotor area F2 of the macaque monkey. J Neurophysiol. 92(4):1990-2002.

877

878   Rathelot JA, Strick PL. 2008. Subdivisions of primary motor cortex based on cortico-motoneuronal
879   cells. Proc Natl Acad Sci U S A. 106(3):918-23.
880

881   Rech F, Herbet G, Moritz-Gasser S, Duffau H. 2016. Somatotopic organization of the white matter
882   tracts underpinning motor control in humans: an electrical stimulation study. Brain Struct Funct.
883   221(7):3743-53.
884

885   Rech F, Duffau H, Pinelli C, Masson A, Roublot P, Billy-Jacques A, Brissart H, Civit T. 2017.
886   Intraoperative identification of the negative motor network during awake surgery to prevent deficit
887   following brain resection in premotor regions. Neurochirurgie. 63(3):235-242.
888

889   Riva M, Fava E, Gallucci M, Comi A, Casarotti A, Alfiero T, Raneri FA, Pessina F, Bello L. 2016.
890   Monopolar high-frequency language mapping: can it help in the surgical management of gliomas? A
891   comparative clinical study. J Neurosurg. 124(5):1479-89.
892

893   Rosett J. 1933. Intercortical Systems of the Human Cerebrum. Columbia University Press, New York.
894

895   Rossi M, Fornia L, Puglisi G, Leonetti A, Zuccon G, Fava E, Milani D, Casarotti A, Riva M, Pessina
896   F, Cerri G, Bello L. 2018. Assessment of the praxis circuit in glioma surgery to reduce the incidence
897   of postoperative and long-term apraxia: a new intraoperative test. J Neurosurg. 23:1-11.
898

899   Stepniewska I, Preuss TM, Kaas JH. 1993. Architectonics, somatotopic organization, and ipsilateral
900   cortical connections of the primary motorarea (M1) of owl monkeys. J Comp Neurol. 330:238 –271.
901

902   Stepniewska I, Preuss TM, Kaas JH. 2006. Ipsilateral cortical connections of dorsal and ventral
903   premotor areas in New World owl monkeys. J Comp Neurol. 495:691–708.
904

905   Strick PL, Preston JB. 1992. Two representations of the hand in area 4 of a primate. II. Somatosensory
906   input organization. J Neurophysiol. 48(1):150-9.
907

908   Tadel F, Baillet S, Mosher JC, Pantazis D, Leahy RM. 2011. Brainstorm: a user-friendly application
909   for MEG/EEG analysis. Comput Intell Neurosci. 2011:879716.
910

Thompson A, Murphy D, Dell'Acqua F, Ecker C, McAlonan G, Howells H, Baron-Cohen S, Lai MC, Lombardo MV; MRC AIMS Consortium, and Marco Catani. 2017. Impaired communication between the motor and somatosensory homunculus is associated with poor manual dexterity in autism spectrum disorder. Biol Psychiatry. 81(3):211-219.

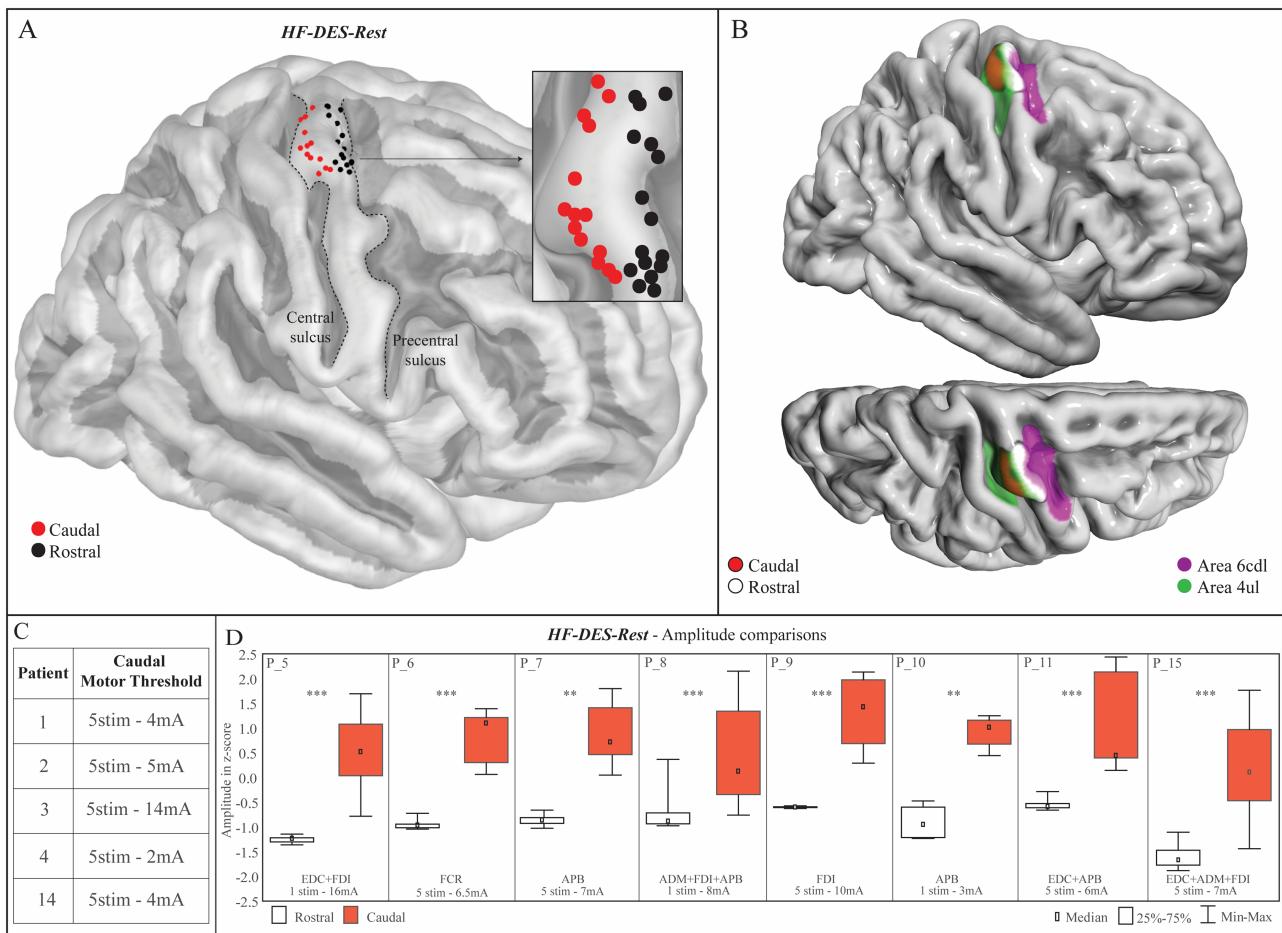Walhovd KB, Johansen-Berg H, Káradóttird RT. 2014. Unraveling the secrets of white matter – Bridging the gap between cellular, animal and human imaging studies. Neuroscience. 276(100): 2–13.
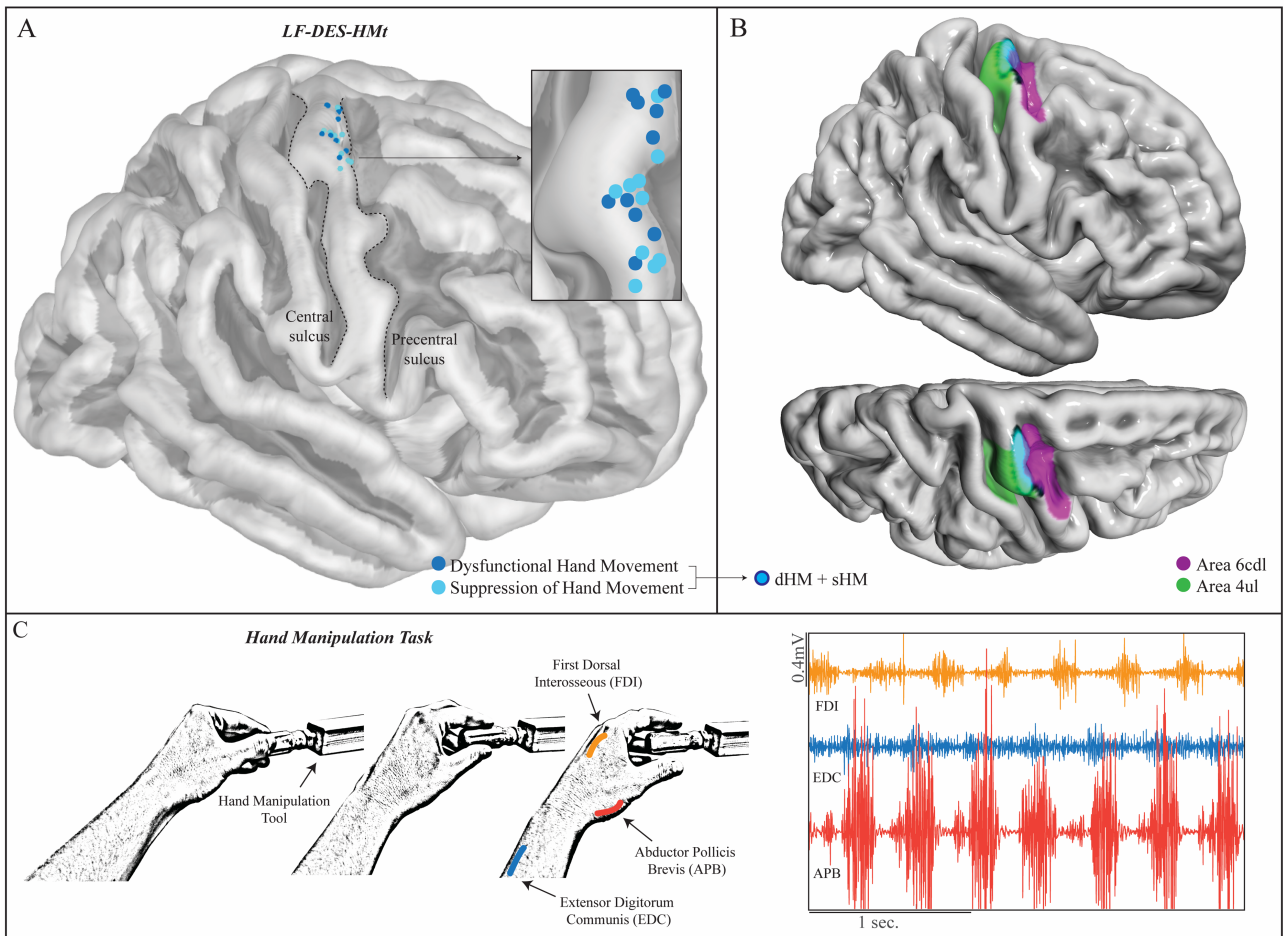
Witham CL, Fisher KM, Edgley SA, Baker SN. 2016. Corticospinal inputs to primate motoneurons innervating the forelimb from two divisions of primary motor cortex and area 3a. J Neurosci. 36(9):2605-16.

Yousry TA, Schmid UD, Alkadhi H, Schmidt D, Peraud A, Buettner A, Winkler P. 1997. Localization of the motor hand area to a knob on the precentral gyrus. A new landmark. Brain. 1:141-57.
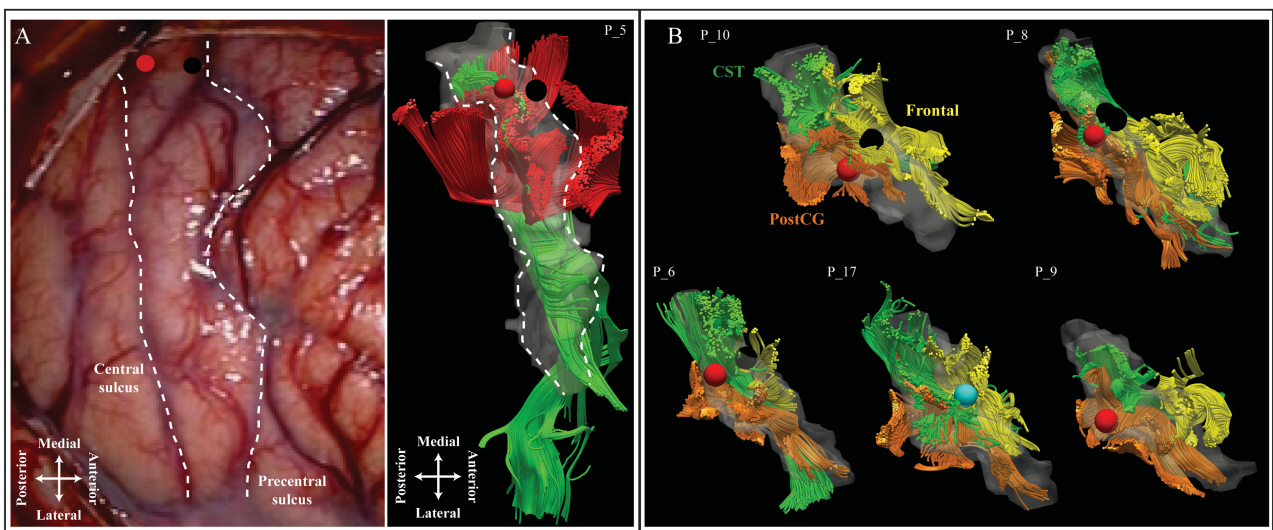
Fig. 1

928   **Fig.2**
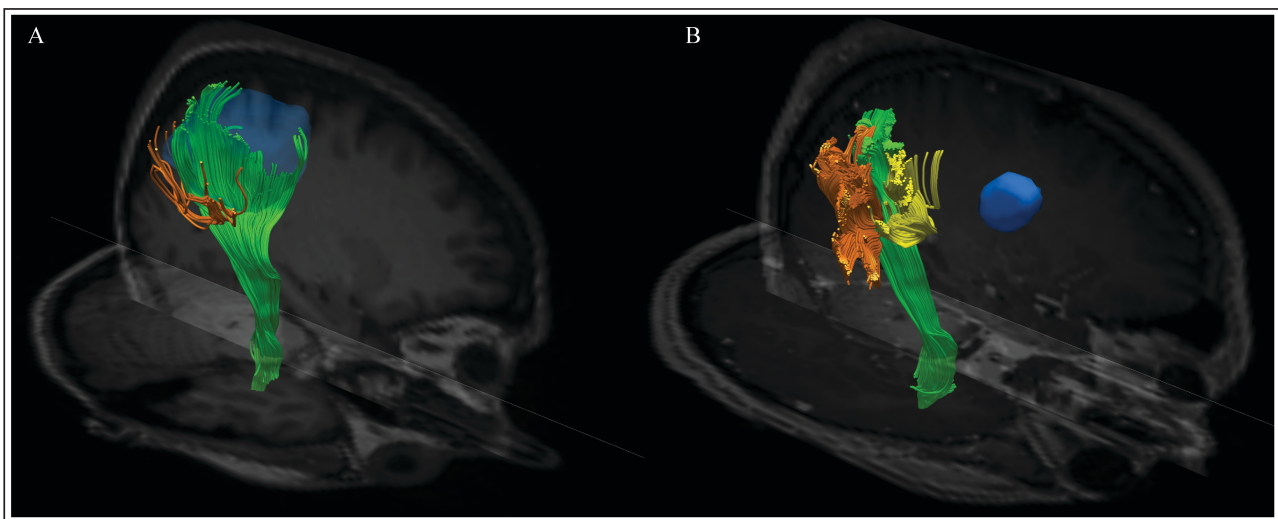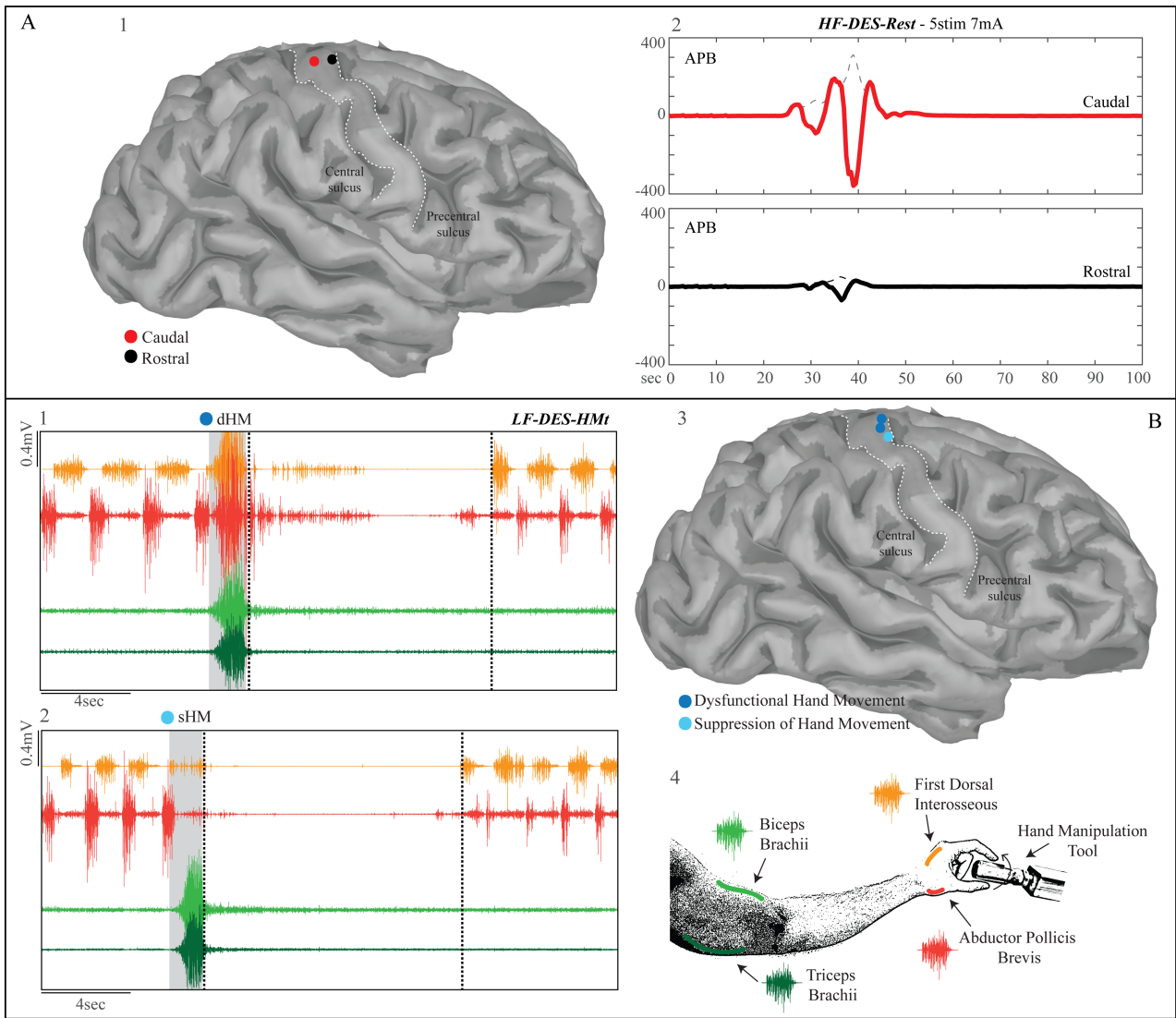

A   *LF-DES-HMt*

B

● Dysfunctional Hand Movement
● Suppression of Hand Movement   → ● dHM + sHM

Central sulcus
Precentral sulcus

● Area 6cdl
● Area 4ul

C   *Hand Manipulation Task*

First Dorsal Interosseous (FDI)

Hand Manipulation Tool

Abductor Pollicis Brevis (APB)

Extensor Digitorum Communis (EDC)

0.4mV

FDI

EDC

APB

1 sec.

929

930

931   **Fig. 3**

A   P_5

Central sulcus
Precentral sulcus

Medial
Posterior   Anterior
Lateral

Medial
Posterior   Anterior
Lateral

B   P_10   P_8

CST
Frontal
PostCG

P_6   P_17   P_9

932

933

934

935 **Fig. 4**

936

937 **Fig. 5**

938

Caption

Fig. 1: A) Cortical distribution of the HF-DES-Rest sites on caudal sector (red) and rostral sector (black) of the hand-knob on the 3D FSAverage template. **B)** Probability density estimation of the two HF-DES-Rest subsectors (caudal hand-knob in red and rostral hand-knob in white). The green and purple rois represent right area 4 (upper limb region) and right caudal dorsolateral area 6 respectively (Fan et al. 2016). **C)** Caudal Motor Threshold (cMT, see Materials and Methods) parameters (number of pulses and intensity) that, applied to the rostral sector of hand-knob failed to elicit motor responses within the same patients. **D)** Comparison of MEP amplitude evoked with the same stimulation parameters (number of pulses and intensity) in the caudal and rostral hand-knob. All MEP amplitude values were standardised within the area and between muscles. Boxplots indicate the median value (small rectangles), 25th-75th (edge of the box) and the most extreme data points (whiskers). $^{*}p < 0.5$; $^{**}p < 0.01$; $^{***}p < 0.001$.

Fig.2: A) Distribution of the cortical stimulation sites associated with the two behavioural outcomes mapped on the 3D FSAverage template: Dysfunctional Hand Movement (blue) and Suppression of hand movement (pale-blue).
B) Probability density estimation of dHM and sHM within the rostral hand-knob. The green and purple rois represent right area 4 (upper limb region) and right caudal dorsolateral area 6 respectively (Fan et al. 2016). **C)** Schematic representation of the HMt execution (left). Example of EMG activity from three hand muscles recorded during HMt execution (APB, Abductor Pollicis Brevis; FDI, First Dorsal Interosseous; EDC, Extensor Digitorum Communis) (right).

Fig. 3: A) 1: Cortical distribution of the HF-DES-Rest sites on the caudal sector (red) and rostral sector (black) of the hand-knob on the 3D MNI brain reconstruction of patient 7. **2**: MEP average of 10 trials elicited by stimulating caudal (red) and rostral (black) hand-knob. The grey dashed lines represent the MEP root mean square. The 10 trials for averaging were selected among a sequence obtained over the same site in the same run. **B) 1**: Example of single trial LF-DES-HMt stimulation resulted in a Dysfunctional Hand Movement. **2**: Example of a single trial LF-DES-HMt stimulation that resulted in a Suppression of Hand Movement coupled with a proximal muscles recruitment. In both (1) and (2) the EMG recording shows 2 hand-muscles (APB and FDI) and 2 proximal muscles (Biceps Brachii and Triceps Brachii). The grey shadow represents the onset and the offset of the stimulations. The time that the patient needed to restore HMt execution is shown between dashed lines. Note that the mere proximal muscles recruitment induced by the stimulation is not a sufficient cause to determine a loss of activity in the hand-muscle district. In fact, a proximal recruitment during dHM could occur simultaneously to distal muscle activation without any inhibition. This led us to characterize sHM as a specific response defined by the suppression of the hand-fingers movements. **3**: Distribution of the cortical stimulation sites associated to the two Behavioural Outcomes mapped on the 3D MNI brain reconstruction of patient 7: Dysfunctional Hand Movement (blue) and Suppression of Hand Movement (pale-blue). **4**: Schematic representation of the HMt execution.

Fig. 4: A) Anatomical localisation of the rostral (black) and caudal (red) HF-DES-Rest stimulation sites in a single patient (5) shown on the intraoperative photograph of the area under the surgical flap (left panel). The black dot represents also the LF-DES-HMt stimulation site on the rostral sector. Diffusion tractography reconstruction (central panel) of connectivity of the precentral gyrus in this patient illustrates corticofugal tracts (green), precentral-postcentral tracts and intra-frontal tracts in red. These connections form a 'poppy flower' formation, described in Catani et al. (2012). **B)** Diffusion tractography reconstruction of corticofugal (green), precentral/postcentral (orange) and

precentral/frontal (yellow) tracts of each single subject plotted in the 3D native space. All the stimulation sites have a diameter of 5mm (Haglund et al. 1993). Red and black dots represent respectively caudal and rostral HF-DES-Rest sites. In patient 17 is shown the anatomical localisation of LF-DES-HMt site of stimulation resulted in a suppression of the hand movement (sHM).

Supplementary

Fig. 5: A) Example of a patient excluded from the study. The volume of the lesion (blue), computed on volumetric fluid-attenuated inversion recovery (FLAIR) MRI scan, occupies the whole hand-knob region infiltrating/dislocating the corticofugal tract (green) and U-shaped cortico-cortical tracts (in orange the precentral/postcentral tracts). The premotor U-shaped tracts are not visible as the diffusion algorithm is unable to track within the tumour. **B)** Example of a patient included in the study (P_9). The lesion (blue), segmented on volumetric fluid-attenuated inversion recovery (FLAIR) MRI scan, is localized in the superior frontal gyrus not infiltrating/dislocating the region of interest and its long- and short-range projection tracts. The distance between the posterior border of the tumour and the precentral sulcus is > 10mm (Quiñones-Hinojosa et al. 2003; Fornia et al. 2016).

Video 1: Example of dysfunctional hand movement (dHM) in P_7 consisted in a closure of the hand on the handle of the tool (see Fig. 3B-1 for the EMG pattern during the stimulation).

Video 2: Example of dysfunctional hand movement (dHM) in P_6 consisted in an aperture of the hand.

Video 3: Example of suppression of hand movement (sHM) in P_11.

Video 3: Example of suppression of hand movement (sHM) in P_7 coupled with proximal (biceps and triceps) involuntary recruitment (see Fig. 3B-2 for the EMG pattern during the stimulation).